
This is an electronic reprint of the original article.
This reprint may differ from the original in pagination and typographic detail.

Author(s): Gogova, D. & Kasic, A. & Larsson, H. & Hemmingsson, C. & Monemar, B. & Tuomisto, Filip & Saarinen, K. & Dobos, L. & Pecz, B. & Gibart, P. & Beaumont, B.

Title: Strain-free bulk-like GaN grown by hydride-vapor-phase-epitaxy on two-step epitaxial lateral overgrown GaN template

Year: 2004

Version: Final published version

Please cite the original version:

Gogova, D. & Kasic, A. & Larsson, H. & Hemmingsson, C. & Monemar, B. & Tuomisto, Filip & Saarinen, K. & Dobos, L. & Pecz, B. & Gibart, P. & Beaumont, B. 2004. Strain-free bulk-like GaN grown by hydride-vapor-phase-epitaxy on two-step epitaxial lateral overgrown GaN template. *Journal of Applied Physics*. Volume 96, Issue 1. 799-806. ISSN 0021-8979 (printed). DOI: 10.1063/1.1753073

Rights: © 2004 American Institute of Physics. This article may be downloaded for personal use only. Any other use requires prior permission of the authors and the American Institute of Physics. The following article appeared in *Journal of Applied Physics*, Volume 96, Issue 1 and may be found at <http://scitation.aip.org/content/aip/journal/jap/96/1/10.1063/1.1753073>.

All material supplied via Aaltodoc is protected by copyright and other intellectual property rights, and duplication or sale of all or part of any of the repository collections is not permitted, except that material may be duplicated by you for your research use or educational purposes in electronic or print form. You must obtain permission for any other use. Electronic or print copies may not be offered, whether for sale or otherwise to anyone who is not an authorised user.

Strain-free bulk-like GaN grown by hydride-vapor-phase-epitaxy on two-step epitaxial lateral overgrown GaN template

D. Gogova, A. Kasic, H. Larsson, C. Hemmingsson, B. Monemar, F. Tuomisto, K. Saarinen, L. Dobos, B. Pécz, P. Gibart, and B. Beaumont

Citation: *Journal of Applied Physics* **96**, 799 (2004); doi: 10.1063/1.1753073

View online: <http://dx.doi.org/10.1063/1.1753073>

View Table of Contents: <http://scitation.aip.org/content/aip/journal/jap/96/1?ver=pdfcov>

Published by the [AIP Publishing](#)

Articles you may be interested in

Time-resolved photoluminescence, positron annihilation, and Al_{0.23}Ga_{0.77}N/GaN heterostructure growth studies on low defect density polar and nonpolar freestanding GaN substrates grown by hydride vapor phase epitaxy

J. Appl. Phys. **111**, 103518 (2012); 10.1063/1.4717955

Exciton localization on basal stacking faults in a -plane epitaxial lateral overgrown GaN grown by hydride vapor phase epitaxy

J. Appl. Phys. **105**, 043102 (2009); 10.1063/1.3075596

Thermal stability of in-grown vacancy defects in GaN grown by hydride vapor phase epitaxy

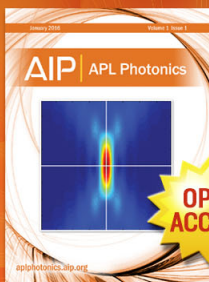
J. Appl. Phys. **99**, 066105 (2006); 10.1063/1.2180450

Ga vacancies as dominant intrinsic acceptors in GaN grown by hydride vapor phase epitaxy

Appl. Phys. Lett. **82**, 3433 (2003); 10.1063/1.1569414

Time-resolved microphotoluminescence of epitaxial laterally overgrown GaN

Appl. Phys. Lett. **75**, 3647 (1999); 10.1063/1.125416



Launching in 2016!

The future of applied photonics research is here

OPEN ACCESS

AIP | APL Photonics

Strain-free bulk-like GaN grown by hydride-vapor-phase-epitaxy on two-step epitaxial lateral overgrown GaN template

D. Gogova,^{a)} A. Kasic,^{b)} H. Larsson, C. Hemmingsson, and B. Monemar
Department of Physics and Measurement Technology, Linköping University, S-58183 Linköping, Sweden

F. Tuomisto and K. Saarinen
Laboratory of Physics, Helsinki University of Technology, P.O. Box 1100, 02015 HUT, Finland

L. Dobos and B. Pécz
Research Institute for Technical Physics and Materials Science of the Hungarian Academy of Science, 1121 Budapest, Hungary

P. Gibart and B. Beaumont
LUMILOG, 2720, Chemin de Saint Bernard, Les Moulins I, F-06220 Vallauris, France

(Received 12 January 2004; accepted 1 April 2004)

Crack-free bulk-like GaN with high crystalline quality has been obtained by hydride-vapor-phase-epitaxy (HVPE) growth on a two-step epitaxial lateral overgrown GaN template on sapphire. During the cooling down stage, the as-grown 270- μm -thick GaN layer was self-separated from the sapphire substrate. Plan-view transmission electron microscopy images show the dislocation density of the free-standing HVPE-GaN to be $\sim 2.5 \times 10^7 \text{ cm}^{-2}$ on the Ga-polar face. A low Ga vacancy related defect concentration of about $8 \times 10^{15} \text{ cm}^{-3}$ is extracted from positron annihilation spectroscopy data. The residual stress and the crystalline quality of the material are studied by two complementary techniques. Low-temperature photoluminescence spectra show the main neutral donor bound exciton line to be composed of a doublet structure at 3.4715 (3.4712) eV and 3.4721 (3.4718) eV for the Ga- (N-) polar face with the higher-energy component dominating. These line positions suggest virtually strain-free material on both surfaces with high crystalline quality as indicated by the small full width at half maximum values of the donor bound exciton lines. The $E_1(\text{TO})$ phonon mode position measured at 558.52 cm^{-1} (Ga face) by infrared spectroscopic ellipsometry confirms the small residual stress in the material, which is hence well suited to act as a lattice-constant and thermal-expansion-coefficient matched substrate for further homoepitaxy, as needed for high-quality III-nitride device applications. © 2004 American Institute of Physics. [DOI: 10.1063/1.1753073]

I. INTRODUCTION

There is currently a great demand in the computer and telecommunication industries for multicolor light emitting displays as well as for high-storage capacities of data in communication and recording systems. The III nitrides are highly suitable for such applications due to their unique electronic and optical properties. Efficient short-wavelength laser diodes emitting in the blue and ultraviolet regions have already been fabricated on the basis of III nitrides and will be employed to achieve the high-storage capacities for the next-generation multimedia systems.

A crucial prerequisite for the effective employment of the III nitrides in device applications is the availability of high-quality crystals with low concentrations of electrically and optically active defects. Heteroepitaxially grown GaN crystals usually suffer from considerable strain and high dislocation densities (10^8 – 10^{10} cm^{-2}) due to the lack of

lattice-constant and thermal-expansion-coefficient matched substrate materials. The dislocation density, however, constitutes a serious limitation for the electron mobility and the efficiency of radiative recombination, and may cause other problems related to the device performance and operating lifetime. The dislocation density can be decreased into the 10^7 cm^{-2} range by means of sophisticated techniques, such as epitaxial lateral overgrowth (ELO)¹ and pendeoepitaxy,² which have been developed in the last decade. Alternatively, a reduction of the dislocation density can be achieved by homoepitaxial growth of GaN.³ Thus, a few years ago, it was realized that high-quality bulk GaN is needed as substrate material to promote large-scale production of different electronic and optoelectronic devices with a high yield from the total wafer area. Based on homoepitaxial GaN, which has been grown involving ELO and hydride-vapor-phase-epitaxy (HVPE) material, high-power and long-lifetime laser diode structures have already been demonstrated.⁴ Furthermore, the availability of GaN substrates will eliminate the need for buffer layers for growth of device structures and provide significant advantages like vertical conduction, heat sinking, and cleavability.

^{a)}Permanent address: Central Laboratory of Solar Energy and New Energy Sources at the Bulg. Acad. Sci., Blvd. Tzarigradsko shose 72, 1784 Sofia, Bulgaria.

^{b)}Author to whom correspondence should be addressed; electronic mail: aleka@ifm.liu.se

Bulk GaN has been grown by different growth techniques, such as the high-temperature, high-pressure, near-equilibrium growth method,⁵ the ammonothermal method,⁶ and the sodium flux method.⁷ However, the high-temperature, high-pressure growth of bulk GaN is able to produce crystal platelets in the range of a centimeter in lateral scale only. This is a considerable limitation for an effective device fabrication despite the low dislocation density achievable for that material. The ammonothermal and sodium flux techniques have demonstrated material of high quality as well, but the lateral size of these crystals is limited even to millimeters. On the other hand, HVPE has proven to be the key technique for cost-effective and large-scale manufacturing of GaN substrates^{8,9} due to its high growth rates. The HVPE grown thick layers once removed from the foreign substrate can serve as lattice-matched and thermally matched substrates for further homoepitaxial growth of high-quality GaN and III-nitride multilayer structures with a low dislocation density, as needed for advanced heterostructure devices.

We have developed a HVPE process for growth of bulk-like GaN in a radio-frequency heated vertical atmospheric-pressure reactor with a bottom-fed design.⁹ Bulk-like GaN with a thickness of 270 μm was grown on a two-step ELO (2S-ELO) GaN template^{1,10} exploiting the advantages of the ELO and HVPE techniques in order to achieve high-quality bulk-like GaN. Due to a self-separation effect, the GaN became delaminated from the substrate at room temperature, and free-standing bulk-like GaN was obtained. The growth parameters and the results of optical and structural investigations are reported here. A variety of characterization techniques, including transmission electron microscopy (TEM), high-resolution x-ray diffraction (HRXRD), low-temperature photoluminescence (PL), low-temperature cathodoluminescence (CL) imaging, infrared spectroscopic ellipsometry (IRSE), and positron annihilation spectroscopy were employed to study in a comparative way the structural and optical quality of the bulk-like material.

II. EXPERIMENT

A. Growth

So far, most of the HVPE growth of GaN has been performed using horizontal growth reactors. The structural, electrical, and optical properties of HVPE-GaN layers strongly depend on the growth conditions, which vary considerably with the reactor design. In this study we employ a vertical HVPE reactor with a bottom-fed design at Linköping University. More technological details can be found in Ref. 9.

Prior to the HVPE growth, the template consisting of a $\sim 10\text{-}\mu\text{m}$ -thick two-step ELO (2S-ELO) GaN layer^{1,10} grown on a sapphire substrate (LUMILOG, France) was heated up to the growth temperature in ammonia atmosphere in order to protect it from decomposition. The GaN was grown as a result of the reaction between ammonia and GaCl gas in the high-temperature zone of the reactor (1090 °C). The GaCl was formed at lower temperature, 850 °C, in the first reactor zone by interaction of liquid Ga with HCl gas.

The HVPE-GaN was grown at 20 ml/min flow rate of HCl gas and at a V:III ratio of 24, i.e., at gallium rich conditions, and using a total gas flow rate of approximately 3 l/min. Nitrogen was employed as carrier gas. The growth was carried out at a temperature of 1090 °C with a growth rate of 68 $\mu\text{m/h}$. The grown bulk-like GaN sample was cooled down to room temperature by temperature ramping with steps of 5K/min, and the effect of self-separation of the layer from the substrate was observed at room temperature.

B. Characterization techniques

Cathodoluminescence (CL) images of the sample cross section were taken at 4.6 K in a Leo 1550 Gemini scanning electron microscope with a MonoCL system (Oxford Instruments) using a 1800 lines/mm grating blazed at 500 nm. A Peltier-cooled photomultiplier was used for detection.

XRD measurements were carried out employing a Philips MRD system with a Cu $K\alpha 1$ ($\lambda = 1.54 \text{ \AA}$) radiation source. For the high-resolution x-ray experiments the triple axis configuration was used, including a Ge(220) monochromator and an analyzer crystal in the front of the detector, providing an instrumental resolution of less than 15 arcsec. The slit width used was 1.5 mm.

Plan-view specimens were prepared for transmission electron microscopy (TEM) studies by Ar^+ ion milling. Small pieces of the GaN sample were cut and embedded in special Ti grids. The embedded pieces were ground with diamond paste and subsequently thinned by 10 keV Ar^+ bombardment in a Technoorg-Linda ion miller. In order to minimize artificial amorphization, the samples were finally bombarded at 3 keV. The transparent specimens were investigated in a Philips CM 20 electron microscope operating at 200 kV.

Positron lifetime experiments were performed in the conventional way by sandwiching two identical samples with a thin ^{22}Na positron source.^{11,12} The energetic positrons emitted from ^{22}Na have a mean penetration depth of about 40 μm in GaN. About 2×10^6 positron annihilation events were collected at temperatures 10–450 K using a spectrometer with a time resolution of 250 ps. After correcting for the background events and annihilations in the source material, the spectra were analyzed by fitting a sum of experimental decay components $\sum I_i \exp(-t/\tau_i)$ convoluted with the Gaussian resolution function. The intensities I_i and lifetime components τ_i were used to calculate the average positron lifetime as $\tau_{\text{ave}} = \sum I_i \tau_i$.

Photoluminescence (PL) experiments were conducted in a He-bath cryostat at 2 K using excitation by the 244 nm line from a frequency doubled Ar^+ laser. The PL emission was dispersed by a 0.46 m single monochromator (Jobin Yvon HR460) with a spectral resolution of about 0.25 meV in the GaN band gap range and detected by a charged-coupled-device camera.

Infrared spectroscopic ellipsometry (IRSE) measurements in reflection mode were performed at room temperature using a Fourier-transform-based spectroscopic ellipsometer equipped with a rotating polarizer and a rotating compensator. The IR probe beam was focused to a spot size

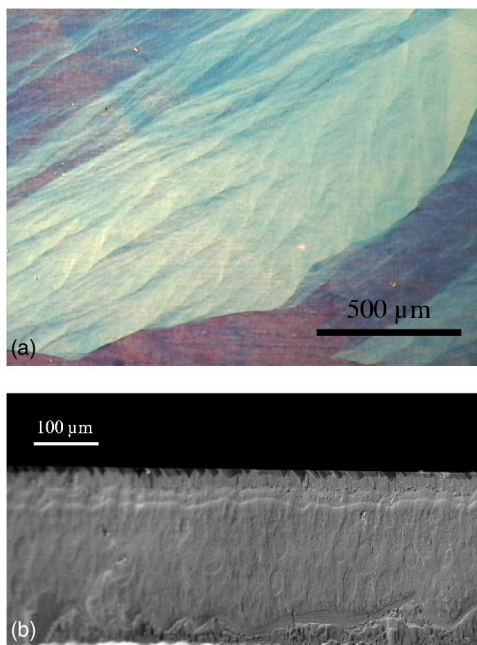


FIG. 1. (a) Optical micrograph from the Ga face of the free-standing HVPE-GaN layer grown on ELO GaN template. (b) Scanning electron microscopy image of the sample cross section. Both images reveal crack-free material.

at the sample surface of $\sim 8 \times 5 \text{ mm}^2$ for the angles of incidence used. Due to the geometry of the experiment, the IRSE data are sensitive to the transverse-optical (TO) mode of E_1 symmetry and the longitudinal-optical (LO) mode of A_1 symmetry. The spectra were taken at multiple angles of incidence (60° , 65° , 70°) and analyzed using an anisotropic factorized model dielectric function ϵ_j ($j = \perp, \parallel$, i.e., perpendicular and parallel to the c axis, respectively) allowing for possible coupling of free-carrier-plasmon excitations with LO phonons. Details of the ellipsometric data analysis can be found elsewhere.¹³

III. RESULTS AND DISCUSSION

A. Structural properties

On visual inspection, the present HVPE bulk-like GaN appeared highly uniform and transparent. Observations done with an optical microscope with Nomarski interference contrast ($50\times$ magnification) reveal the morphology of the Ga-polar surface without any visible surface defects and cracks. A typical optical micrograph is illustrated in Fig. 1(a). The absence of cracks in the HVPE material is confirmed by scanning electron microscopy images of the sample cross section [Fig. 1(b)].

Low-temperature cross-sectional CL spectroscopy and imaging allows visualization of regions with different luminescent properties revealing features not detectable by plan-view images. In order to gain insight into the evolution of the structural properties of the GaN sample along the growth direction we have examined it in cross section by CL. For comparison, we first show [Fig. 2(a)] a panchromatic CL image typical of a bulk-like GaN layer grown on a bare sapphire substrate, i.e., without using a 2S-ELO GaN template. This HVPE-GaN layer was deposited at a growth rate

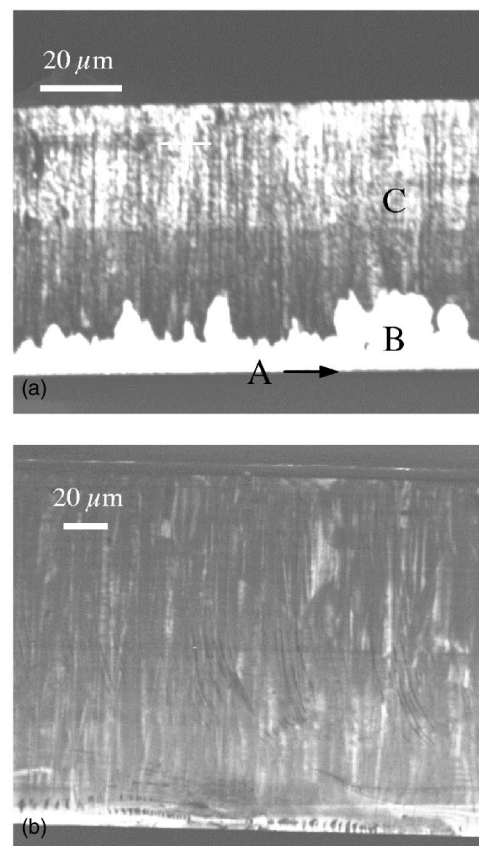


FIG. 2. Panchromatic CL image (a) of a HVPE-GaN layer grown directly on sapphire and (b) of the HVPE-GaN layer grown on ELO-GaN template.

similar to that used for the sample grown on the 2S-ELO GaN template. Three different structural areas can be clearly observed, which are characteristic of the growth without buffer layers. The first one (A) is a highly defective nonradiative nucleation layer with a thickness of about $1 \mu\text{m}$, which is formed in result of nitridation and GaCl pretreatment of the sapphire substrate. The second one (B) is a columnar grown bright-emission region, and the third one (C) constitutes the high-quality zone of the GaN. Mismatch-induced lattice strain causes the formation of the highly defective layer at the GaN/sapphire interface. The material in region B shows larger PL and CL linewidths and brighter CL emission than that in zone C, most likely due to a high oxygen content, which may originate from the sapphire substrate. Figure 2(b) illustrates a panchromatic cross-section image of the HVPE-GaN sample grown on the 2S-ELO template.¹⁴ The image was taken at the same conditions as for Fig. 2(a). In contrast to the sample without 2S-ELO template, the CL emission now appears highly homogeneous, revealing a high-quality zone only. Obviously, there is no highly defective columnar area close to the N-polar side as it was observed for the bulk-like GaN grown directly on sapphire [Fig. 2(a)] or for GaN grown on a metal organic chemical vapor deposition (MOCVD)-GaN buffer layer at a very high growth rate.¹⁵

The crystalline quality of the free-standing sample was estimated by the HRXRD rocking curve measurements (ω scans). For the Ga-polar face of our material, the full width

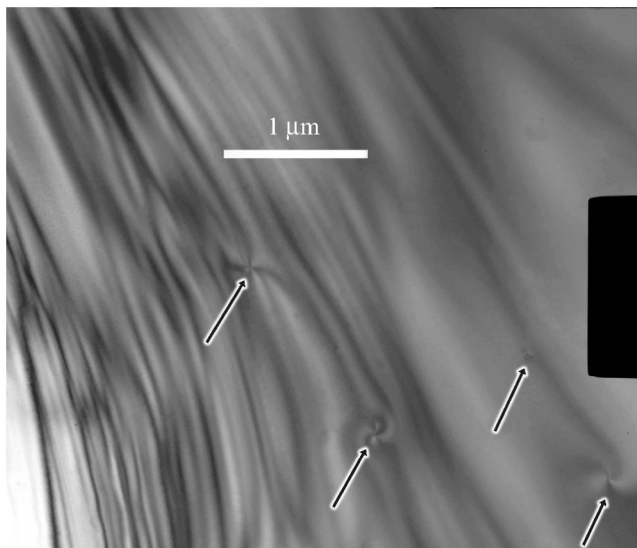


FIG. 3. Plan-view TEM image of the as-grown Ga face. The dislocations intersecting the surface are marked by arrows.

at half maximum (FWHM) values of the (1 0–1 4) and (0 0 0 2) reflections are 254 and 293 arcsec, respectively, while for the N-polar face the respective values are 276 and 310 arcsec. These data show that both the Ga and the N-polar face of our free-standing HVPE-GaN are of high crystalline quality. The ω values obtained compare well to data reported in literature for free-standing HVPE-GaN taking into account the different slit widths used, which remain often unspecified in reports.¹⁶

Figure 3 exhibits a plan-view TEM image of the as-grown Ga face of the free-standing GaN. The dislocations intersecting the surface are marked by arrows. By analyzing different regions of the investigated sample, the dislocation density is estimated to be $2.5 \times 10^7 \text{ cm}^{-2}$, which is close to the value reported for free-standing material produced by Samsung, Korea.¹⁷

Ga vacancies have been observed as important native defects in *n*-type GaN by positron annihilation spectroscopy.¹¹ Positrons get trapped at neutral and negative vacancies because of the missing positive charge of the ion cores. The reduced electron density at vacancies increases the positron lifetime.

The positron lifetime spectrum measured at room temperature in the free-standing GaN [Fig. 4(a)] provides an average lifetime of $\tau_{\text{ave}} = 162 \pm 0.3 \text{ ps}$. Figure 4(a) also shows the spectrum of a homoepitaxial HVPE-GaN reference sample,¹⁸ where the positrons annihilate only in the GaN lattice with the lifetime $\tau_B = 159 \pm 0.3 \text{ ps}$. As can be seen from the figure, at $t \geq 500 \text{ ps}$ the difference $\tau_{\text{ave}} - \tau_B = 3 \text{ ps}$ is statistically significant. The lifetime component resulting from positrons annihilating as trapped at vacancies could be decomposed from the data measured at 300–450 K in free-standing GaN, giving $\tau_2 = 240 \pm 25 \text{ ps}$. This lifetime can be attributed to the Ga vacancy.¹⁹ The Ga vacancy concentration can be estimated as $[V_{\text{Ga}}] = (8 \pm 2) \times 10^{15} \text{ cm}^{-3}$ from the positron trapping model¹¹ using the vacancy related lifetime τ_2 together with the difference $\tau_{\text{ave}} - \tau_B = 3 \text{ ps}$. This

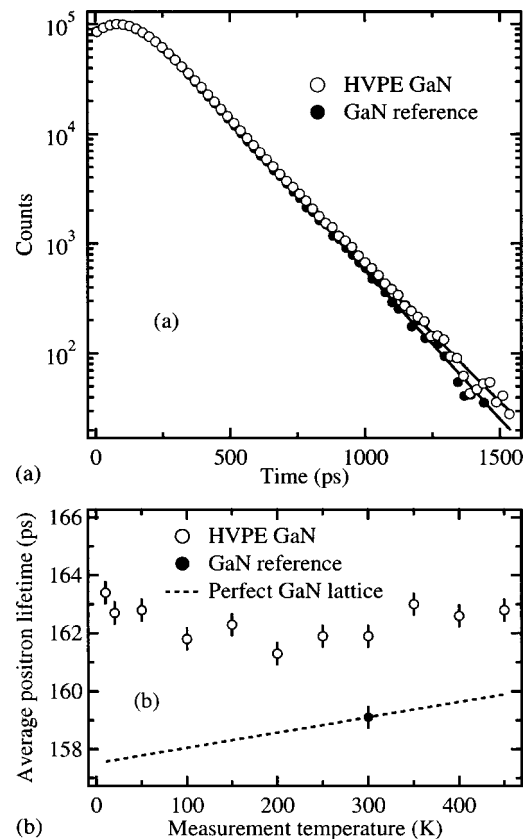


FIG. 4. (a) Positron lifetime spectra at 300 K measured in the HVPE-GaN sample and a GaN reference sample, where no positron trapping at vacancies is observed (see Ref. 18). The solid lines are fits of exponential decay components to the data. The background events and the positron annihilations in the source have been subtracted from the data. (b) The positron lifetime measured in HVPE-GaN as a function of measurement temperature. The dashed line describes the effect of the thermal expansion on the positron lifetime in the GaN lattice observed in bulk GaN:Mg (see Ref. 12).

is similar to the vacancy concentrations observed in HVPE-GaN layers of similar thickness grown directly on sapphire.^{20,21} From Fig. 4(b) it can be seen that with decreasing temperature, the average positron lifetime increases below 200 K. This indicates enhanced positron trapping at V_{Ga} and shows that the observed Ga vacancies are in the negative charge state. In agreement with previous studies,²⁰ the Ga vacancy or complexes involving V_{Ga} and oxygen are thus one of the dominant acceptor defects in HVPE-GaN.

B. Optical properties

The crystalline quality and the residual stress in the present bulk-like GaN sample were evaluated by low-temperature photoluminescence measurements. A typical near-band gap PL spectrum taken on the Ga face is shown in Fig. 5(a). The PL emission is dominated by a very narrow and intense peak (*d*) with a clear asymmetric line shape [see inset in Fig. 5(a)] pointing to the participation of more than one transition. Assuming the existence of two lines, the line shape analysis of peak *d* yields the components d_1 and d_2 at 3.4721 and 3.4715 eV, respectively. The presence of a doublet or multiplet structure in this spectral region has been reported previously^{22,23} and attributed to the ground-state A

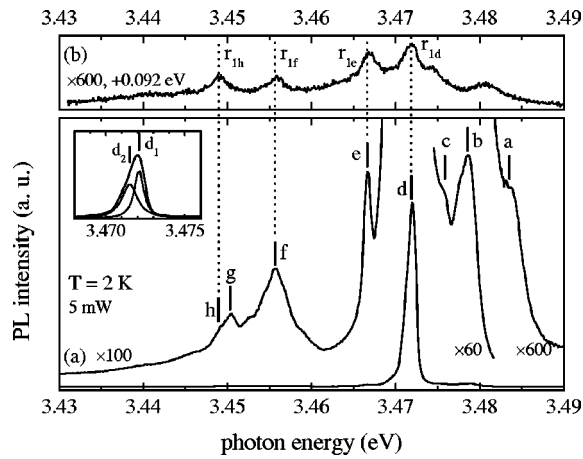


FIG. 5. (a) Near-band gap PL spectrum taken on the Ga face of the free-standing material. The inset gives a detailed view on peak *d*, which is actually composed of a doublet structure. (b) PL spectrum recorded in the range of 1-LO-phonon replicas of the acceptor bound excitons, shifted by +92 meV for direct comparison to the spectrum in (a). See Table I for peak assignment.

exciton bound to different neutral shallow donors, $(D_i^0, X_A^{n=1})$.²⁴ The identity of these donors is not fully settled yet, but according to recent PL studies combined with high-resolution IR measurements and highly sensitive secondary ion mass spectroscopy data²⁵ we suggest the main donor (d_1) in our sample to be Si_{Ga} , in consistence with the experience that this donor does not form complexes with the V_{Ga} .²⁶ The weaker line d_2 may then be related to O_{N} or another unidentified donor. The full width at half maximum (FWHM) values of peaks d_1 and d_2 are 0.71 and 1.19 meV confirming a high degree of crystalline quality of the material grown. The position of the doublet peak (d_1, d_2) lies close to the range of values reported for the main donor bound exciton in free-standing GaN (3.4720 eV),²⁷ homoepitaxial (3.4709 eV^{28,22} and 3.4718 eV²²), and bulk GaN (3.4712 eV),²⁹ all of which are considered as virtually unstrained.

For the N-polar face, the components d_1 and d_2 are observed at 3.4718 and 3.4712 eV with FWHM values of 1.21 and 1.53 meV (not shown). These line broadening values indicate an only slightly deteriorated structural quality with respect to the Ga face, which is in striking contrast to observations on GaN layers grown directly on sapphire, where the N-polar face typically exhibits a considerably worse structural quality than the Ga face,^{21,16} primarily due to the large lattice mismatch with the substrate. In accordance with the results from the low-temperature CL studies [Fig. 2(b)] and with the HRXRD data, the structural quality of both faces is obviously similar in the present sample. This is mainly due to the properties of the 2S-ELO GaN material present at the N face.

The other emission lines ($a-c, e-h$) observed in the PL spectrum in the 3.44–3.49 eV region and their tentative assignments are summarized in Table I. As the LO phonon coupling strength of acceptor bound excitons is relatively strong in polar semiconductors,³⁰ the acceptor related excitonic transitions can be readily identified by their strong LO

TABLE I. Spectral PL features detected in the near-band gap range and in interesting lower-energy regions for the Ga face and their most plausible assignments.

Peak	Energy (eV)	Assignment
<i>a</i>	3.4840	$X_B^{n=1}$
<i>b</i>	3.4789	$X_A^{n=1}$
<i>c</i>	3.4756	$(D_1^0, X_B^{n=1})$
d_1	3.4721	$(D_1^0, X_A^{n=1}); D_1^0 = \text{Si}_{\text{Ga}}$
d_2	3.4715	$(D_2^0, X_A^{n=1}); D_2^0 = \text{O}_{\text{N}} (?)$
<i>e</i>	3.4666	$(A_1^0, X_A^{n=1}); A_1^0 = \text{Mg}_{\text{Ga}} (?)$
<i>f</i>	3.4557	$(A_2^0, X_A^{n=1}); A_2^0 = \text{Zn}_{\text{Ga}} (?)$
<i>g</i>	3.4504	$(D_1^0, X_A^{n=1})_{2e-}$
<i>h</i>	3.4493	$(A_3^0, X_A^{n=1}); A_3^0$ unknown
<i>j</i>	3.2961	$(X_A^{n=1})^{2-LO}/(e^-, A_4^0)$
<i>k</i>	3.2889	$(D_{1,2}^0, X_A^{n=1})^{2-LO}$
<i>l</i>	3.2631	$(A_4^0, D_3^0); A_4^0 = \text{Mg}_{\text{Ga}}/\text{C}_{\text{N}}/$ structural defects; $D_3^0 = \text{Si}_{\text{Ga}}$
<i>m</i>	2.18	YL, probably C related
<i>n</i>	1.2984	Fe related

phonon replicas. The 1-LO-phonon-assisted transition region of the near-band gap excitonic features is depicted in Fig. 5(b) (features $r_{1d}, r_{1e}, r_{1f}, r_{1h}$). This spectrum is shifted up by +92 meV, in order to align the LO replicas with the corresponding no-phonon transitions. Besides the replica of peak *d*, the replicas of features *e*, *f*, and *h* can clearly be observed suggesting these features being due to shallow acceptor related excitonic transitions [$(A_i^0, X_A^{n=1}), i = 1, 2, 3$]. Transitions *e* and *f* may originate from intrinsic defects rather than from impurities as pointed out by Kirilyuk *et al.* for similar features.³¹ However, PL investigations of intentionally doped HVPE-grown material revealed features, which correspond to transitions *e* and *f* (after appropriate strain consideration) and were hence assigned to Mg and Zn acceptors, respectively.³² The fact that an acceptor bound exciton has been reported to be present close to the position of line *e* in the majority of the HVPE-grown GaN material so far, where Mg is known to be a common contaminant, supports the interpretation of line *e* as being Mg related. A possibly strain dependent binding energy of this acceptor bound exciton,²⁴ however, limits comparability among the observed PL structures in different studies. Therefore, the assignment of both acceptors is only tentative here. Observation of the fairly weak feature *h* has been scarcely reported so far, mainly due to the frequent presence of the usually much stronger adjacent line *g*. A structure similar to feature *h* was observed in MOCVD grown material and was attributed to an unknown donor,³³ which, however, can be excluded here as a possible origin for feature *h* due to its strong LO phonon replica. Line *g* has been widely observed so far, in particular for high-quality homoepitaxial material, and assigned to a two-electron satellite of the main donor bound exciton transition leaving the neutral donor in the excited $2s$ -like state [$(D_1^0, X_A^{n=1})_{2e-}$].²⁸

On the high-energy side of the prominent line *d*, a peak at 3.4756 eV (*c*) can be well resolved. A plausible interpretation of line *c* is emission due to the main donor bound *B* exciton in the ground state, $(D_1^0, X_B^{n=1})$, i.e., the exciton involving a hole from the crystal-field split Γ_7 valence

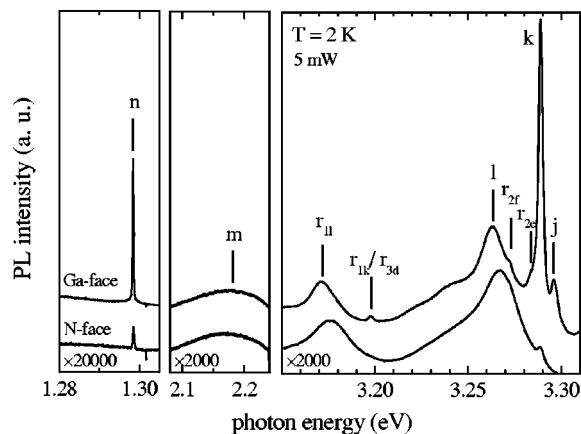


FIG. 6. (a) PL spectra taken on the Ga face (upper curve) and the N face (lower curve) in the range of the donor–acceptor pair recombination, the yellow luminescence band, and the iron related deep level emission. See Table I for peak assignment.

band.^{23,34} However, a recombination process including an excited initial state of the main donor bound exciton complex $[(D_{1,2}^0, X_A)^{n>1}]$ cannot be ruled out. Features *a* and *b* are attributed to the ground state of free *B* exciton ($X_B^{n=1}$) and free *A* exciton ($X_A^{n=1}$), respectively.

Figure 6 displays PL spectra (Ga face) from interesting regions below the near-band gap range. We first consider the region between 3.15 and 3.30 eV that is dominated by a sharp line (*k*) at 3.2889 eV with a FWHM of 2.86 meV. The energetic position of this line coincides with the anticipated 2-LO-phonon replica of the main shallow donor bound exciton transitions ($(D_{1,2}^0, X_A^{n=1})$), but its magnitude is unusually strong compared to the lines observed at the expected positions of the other phonon sidebands of $(D_{1,2}^0, X_A^{n=1})$, as already pointed out previously.³⁵ In the corresponding spectrum of the N-face (lower curve in Fig. 6), the magnitude of peak *k* is strongly reduced and, at the same time, the 1-LO-phonon replica r_{1d} appears considerably decreased with respect to the adjacent 1-LO-phonon replica of the shallow acceptor related excitonic transitions r_{1e} and r_{1f} (not shown). We further experienced that peak *k* is missing whenever the 1-LO-phonon replica r_{1d} vanishes as well, in, e.g., samples of less crystalline quality. Since the appearances of features *k* and r_{1d} are obviously tied up to each other, the assignment of feature *k* to the 2-LO-phonon replica of line *d* is favored. The same assignment has been given for similar strong lines reported previously for undoped, low C- and Be-doped HVPE-grown GaN.^{32,36} Between features *k* and *l*, the weak 2-LO-phonon replicas (r_{2e}, r_{2f}) of the shallow acceptor related excitonic ($(A_1^0, X_A^{n=1})$ and $(A_2^0, X_A^{n=1})$) lines can be detected.

A broad structure (FWHM 15.5 meV) occurs at 3.2631 eV (*l*) in the spectrum of the Ga face. In the case of the N face, this peak is even broader (FWHM 26.4 meV) and slightly shifted up to 3.2680 eV. Such comparatively broad structures have been observed frequently in the range 3.26–3.28 eV in low-temperature PL spectra of GaN, regardless of the growth method and dominating doping species, and attributed to the no-phonon line of a donor–acceptor pair (DAP) recombination process. This assignment has been

concluded from the observation that this transition is subject to characteristic energy shifts in dependence on the excitation intensity, temperature, and doping concentration.^{37,35,38} The nature of the donor and acceptor involved in this emission is not clear though. The appearance of the DAP line has previously been found to be correlated with Mg doping,^{32,39} but the acceptor involved may also be C_N (Ref. 37) suggested to have a binding energy similar to that of the Mg acceptor. Another possibility is the participation of acceptor-like native defects incorporated unintentionally during growth.³⁵ The donor associated with the DAP emission is most probably Si.³⁷ Several LO-phonon sidebands of the DAP transition are observed at lower energies, the first of which (r_{1l}) is shown in Fig. 6. Weak bumps on the low-energy tail of line *l* are strongly connected to the DAP transition³⁵ and are thus likely to arise from acoustic phonon mode replicas of the DAP transition. At 33.0 meV above the DAP line, a small and sharp peak (*j*, FWHM 5.52 meV) is resolved being either due to the 2-LO-phonon replica of the free *A* exciton or the free-electron-to-bound-hole recombination connected with the same acceptor participating in the DAP transition. In the spectrum of the N face, this feature is absent arguing for the former interpretation.

A broad and asymmetric emission band is centered at 2.18 eV (feature *m*) in the spectra from both the Ga and the N face, commonly referred to as yellow luminescence (YL). While this phenomenon has been observed in the large majority of GaN material and thoroughly investigated, its definite identification has yet to be elucidated. Generally, the YL band and other deep-level emissions are regarded as marks of poor crystalline quality. The YL is made up, most probably, of more than one recombination channel involving deep acceptor levels, and recent studies strongly suggest the involvement of C impurities⁴⁰ in addition to the original suggestion of a $V_{Ga}-O$ acceptor complex.^{19,20} Here, we want to emphasize that in our present sample the YL is very weak (note the scaling factor) for both polar surfaces and is hence fully negligible in terms of being a limiting factor for the near-band gap radiative emission efficiency.

The infrared PL range, as shown in the left portion of Fig. 6, is dominated by a sharp emission at 1.2984 eV (feature *n*) that is characteristic of ubiquitous iron trace impurities. The observed line has been assigned previously to an internal no-phonon transition of Fe_{Ga}^{3+} .⁴¹

The optical response of materials in the IR spectral range is able to give information about material quality and internal stress via broadening and frequency of IR active phonon modes. By quantifying free-carrier-plasmon effects, concentration and mobility of free carriers can be determined in the IR frequency range as well. Both phonon and free-carrier properties of the bulk-like HVPE-GaN were investigated by means of IRSE at room temperature. Figures 7(a) and 7(b) show the measured and modeled ellipsometric Ψ and Δ spectra taken on the Ga-polar face of the HVPE-GaN sample in the reststrahlen range. The $E_1(\text{TO})$ phonon mode is located at $558.52 \pm 0.08 \text{ cm}^{-1}$ [see Fig. 7(c)], as obtained from the data regression analysis, where the model parameters were varied until modeled and experimental data match as closely as possible. Employing a hydrostatic linear stress coefficient

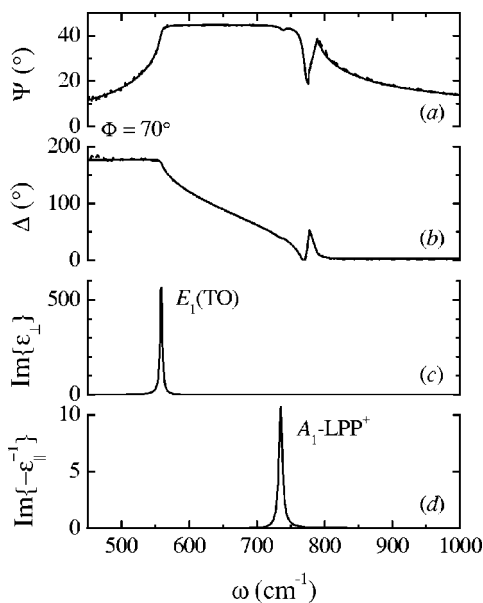


FIG. 7. Mid-IR ellipsometric Ψ (a) and Δ (b) spectra taken on the Ga face. Dashed line, experimental data; solid line, modeled data. (c) Imaginary part of ϵ_{\perp} revealing the $E_1(\text{TO})$ phonon and (d) imaginary part of the dielectric loss function for $j=\parallel$, i.e., parallel to the c axis, where the $A_1\text{-LPP}^+$ mode is peaking. The $\text{Im}\{\epsilon_{\perp}\}$ and $\text{Im}\{-\epsilon_{\parallel}\}$ spectra are gained from the data regression analysis.

of $\partial\omega[E_1(\text{TO})]/\partial\sigma = -3.47 \text{ cm}^{-1}/\text{GPa}$ (Ref. 42) on the basis of experimental phonon deformation potentials reported by Davydov *et al.*⁴³ and elastic constants from Polian, Grimsditch, and Grzegory,⁴⁴ and considering the phonon frequency value reported from Raman scattering measurements on stress-free material,⁴⁵ the residual average stress in the HVPE material close to the Ga face can be estimated to be very slightly compressive, $\sigma = -0.09 (\pm 0.02) \text{ GPa}$. This observation agrees well with the result of the PL studies. The small $E_1(\text{TO})$ mode broadening parameter of $3.22 (\pm 0.14) \text{ cm}^{-1}$, which is similar to that measured for high-quality molecular beam epitaxy (MBE)-grown material,¹³ confirms the high crystalline quality of the HVPE material. The IRSE data analysis further shows that the free-carrier contribution to the IR dielectric response is very weak. In fact, the free-carrier concentration is undeterminable here due to the noticeable uncertainty concerning the frequencies of the uncoupled LO phonons for highly resistive GaN ($A_1: \sim 731\text{--}733 \text{ cm}^{-1}$; $E_1: \sim 738\text{--}741 \text{ cm}^{-1}$). From the frequency of the upper $A_1(\text{LO})$ -phonon plasmon coupled mode branch ($A_1\text{LPP}^+$) determined by IRSE at $732.68 \pm 0.07 \text{ cm}^{-1}$ [see Fig. 7(d)] it can, nevertheless, be concluded that the free-electron concentration in the material is less than $2 \times 10^{17} \text{ cm}^{-3}$.

IV. CONCLUSIONS

High-quality bulk-like GaN with a thickness of $270 \mu\text{m}$ was grown on a 2S-ELO GaN template by HVPE. The bulk-like material, which was self-separated from the sapphire substrate during the cooling down stage to room temperature, has a low dislocation density of $\sim 2.5 \times 10^7 \text{ cm}^{-2}$ on the Ga face revealed by plan-view TEM images. The absence of

cracks is concluded from optical microscopy and scanning electron microscopy images. Using positron annihilation spectroscopy the concentration of Ga vacancy related defects is determined as $\sim 8 \times 10^{15} \text{ cm}^{-3}$. Near-band gap PL studies show that both the Ga- and N-polar face are virtually strain free and of comparable crystalline quality. The latter is consistent with the homogeneous layer depth profile inferred from cross-sectional CL images and is independently confirmed by HRXRD rocking curve measurements. Tentative assignments of residual donor and acceptor related emissions observed by PL are given. The IRSE data analysis confirms the very small material stress on the Ga face and the high crystalline quality of the HVPE-GaN, which is comparable to that of MBE-grown material. The free-standing bulk-like HVPE-GaN presented here can serve as a lattice- and thermal-expansion-coefficient matched substrate for further growth of high-quality III-nitride heterostructures used for advanced electronic and optoelectronic device applications.

ACKNOWLEDGMENTS

The authors thank Dr. I. Ivanov (Linköping University) for performing the PL measurement. A.K. acknowledges support from Wenner-Gren foundation (Sweden). B.P. acknowledges the support of Bolyai Janos Scholarship (Hungary) and OTKAT047141. D.G. says thanks for a scholarship within the Research Training Network CLERMONT funded by the European Commission.

- ¹P. Gibart, B. Beaumont, and P. Vennéguès, in *Nitride Semiconductors Handbook on Materials and Devices*, edited by P. Ruterana, M. Albrecht, and J. Neugebauer (Wiley-VCH, Weinheim, 2003), p. 45.
- ²R. F. Davis, T. Gehrke, K. J. Linthicum, T. S. Zheleva, E. A. Preble, P. Rajagopal, C. A. Zorman, and M. Mehregany, *J. Cryst. Growth* **225**, 134 (2001).
- ³N. Grandjean, B. Damilano, J. Massies, G. Neu, M. Teissere, I. Grzegory, S. Porowski, M. Gallart, P. Lefebvre, B. Gil, and M. Albrecht, *J. Appl. Phys.* **88**, 183 (2000).
- ⁴S. Nagahama, N. Iwasa, M. Senoh, T. Matsushita, Y. Sugimoto, H. Kiyoku, T. Kozaki, M. Sano, H. Matsumura, H. Unemoto, K. Chocho, and T. Mukai, *Jpn. J. Appl. Phys., Part 2* **39**, L647 (2000).
- ⁵J. L. Weyher, M. Albrecht, T. Wosinski, G. Nowak, H. P. Strunk, and S. Porowski, *Mater. Sci. Eng., B* **80**, 318 (2001).
- ⁶D. R. Ketchum and J. W. Kolis, *J. Cryst. Growth* **222**, 431 (2001).
- ⁷T. Iwahashi, F. Kawamura, M. Morishita, Y. Kai, M. Yoshimura, Y. Mori, and T. Sasaki, *J. Cryst. Growth* **253**, 1 (2003).
- ⁸X. Xu, R. P. Vaudo, C. Loria, A. Salant, G. R. Brandes, and J. Chaudhuri, *J. Cryst. Growth* **246**, 223 (2002).
- ⁹D. Gogova, H. Larsson, R. Yakimova, Z. Zolnai, I. Ivanov, and B. Monemar, *Phys. Status Solidi A* **200**, 13 (2003).
- ¹⁰P. Vennéguès, B. Beaumont, V. Bousquet, M. Vaille, and P. Gibart, *J. Appl. Phys.* **87**, 4175 (2000).
- ¹¹K. Saarinen, P. Hautojärvi, and C. Corbel, in *Identification of Defects in Semiconductors*, edited by M. Stavola (Academic, New York, 1998), p. 209.
- ¹²K. Saarinen, J. Nissilä, P. Hautojärvi, J. Likonen, T. Suski, I. Grzegory, B. Lucznik, and S. Porowski, *Appl. Phys. Lett.* **75**, 2441 (1999).
- ¹³A. Kasic, M. Schubert, S. Einfeldt, D. Hommel, and T. E. Tiwald, *Phys. Rev. B* **62**, 7365 (2000).
- ¹⁴The image shown in Fig. 2(b) was taken close to the wafer edge where the thickness of the HVPE-GaN was reduced. Due to the used radial nonsymmetric growth setup the thickness varied between 270 and $170 \mu\text{m}$ over the 2 in. wafer. In the central area, the GaN layer thickness is $\sim 270 \mu\text{m}$, as can be seen in the scanning electron microscopy image of Fig. 1(b).
- ¹⁵A. Kasic, D. Gogova, H. Larsson, C. Hemmingsson, I. Ivanov, R. Yakimova, B. Monemar, and M. Heuken (unpublished).
- ¹⁶H. Morkoç, *Mater. Sci. Eng., R*, **33**, 135 (2001).

- ¹⁷J. Jasinski, W. Swider, Z. Liliental-Weber, P. Visconti, K. M. Jones, M. A. Reshchikov, F. Yun, H. Morkoç, S. S. Park, and K. Y. Lee, *Appl. Phys. Lett.* **78**, 2297 (2001).
- ¹⁸F. Tuomisto, T. Suski, H. Teisseyre, M. Krysko, M. Leszczynski, B. Lucznik, I. Grzegory, S. Porowski, D. Wasik, A. Witowski, W. Gebicki, P. Hageman, and K. Saarinen, *Phys. Status Solidi B* **240**, 289 (2003).
- ¹⁹K. Saarinen, T. Laine, S. Kuisma, J. Nissilä, P. Hautojärvi, L. Dobrzynski, J. M. Baranowski, K. Pakula, R. Stepniowski, M. Wojdak, A. Wyszomolek, T. Suski, M. Leszczynski, I. Grzegory, and S. Porowski, *Phys. Rev. Lett.* **79**, 3030 (1997).
- ²⁰J. Oila, J. Kivioja, V. Ranki, K. Saarinen, D. C. Look, R. J. Molnar, S. S. Park, S. K. Lee, and J. Y. Han, *Appl. Phys. Lett.* **82**, 3433 (2003).
- ²¹D. Gogova, A. Kasic, H. Larsson, B. Pécz, R. Yakimova, B. Magnusson, B. Monemar, F. Tuomisto, K. Saarinen, C. R. Miskys, M. Stutzmann, C. Bundesmann, and M. Schubert, *Jpn. J. Appl. Phys., Part 1* **43**, 1264 (2004).
- ²²M. Mayer, A. Pelzmann, M. Kamp, K. J. Ebeling, H. Teisseyre, G. Nowak, M. Leszczynski, I. Grzegory, S. Porowski, and G. Karczewski, *Jpn. J. Appl. Phys., Part 2* **36**, L1634 (1997).
- ²³J. A. Freitas, Jr., W. J. Moore, B. V. Shanabrook, G. C. B. Braga, S. K. Lee, S. S. Park, and J. Y. Han, *Phys. Rev. B* **66**, 233311 (2002).
- ²⁴B. Monemar, *J. Phys.: Condens. Matter* **13**, 7011 (2001).
- ²⁵J. A. Freitas, Jr., W. J. Moore, B. V. Shanabrook, G. C. B. Braga, D. D. Koleske, S. K. Lee, S. S. Park, and J. Y. Han, *Phys. Status Solidi B* **240**, 330 (2003).
- ²⁶J. Oila, V. Ranki, J. Kivioja, K. Saarinen, P. Hautojärvi, J. Likonen, J. M. Baranowski, K. Pakula, T. Suski, M. Leszczynski, and I. Grzegory, *Phys. Rev. B* **63**, 045205 (2001).
- ²⁷A. Wyszomolek, K. P. Korona, R. Stepniowski, J. M. Baranowski, J. Błoniarczyk, M. Potemski, R. L. Jones, D. C. Look, J. Kuhl, S. S. Park, and S. K. Lee, *Phys. Rev. B* **66**, 245317 (2002).
- ²⁸K. Kornitzer, T. Ebner, K. Thonke, R. Sauer, C. Kirchner, V. Schwegler, M. Kamp, M. Leszczynski, I. Grzegory, and S. Porowski, *Phys. Rev. B* **60**, 1471 (1999).
- ²⁹B. J. Skromme, K. C. Palle, C. D. Poweleit, H. Yamane, M. Aoki, and F. J. DiSalvo, *Appl. Phys. Lett.* **81**, 3765 (2002).
- ³⁰S. Permogorov, in *Modern Problems in Condensed Matter Science*, edited by E. I. Rashba and M. D. Sturge (North-Holland, Amsterdam, 1982), Vol. 2, p. 177.
- ³¹V. Kirilyuk, P. R. Hageman, P. C. M. Christianen, P. K. Larsen, and M. Zielinski, *Appl. Phys. Lett.* **79**, 4109 (2001).
- ³²B. J. Skromme and G. L. Martinez, *MRS Internet J. Nitride Semicond. Res.* **5S1**, W9 (2000).
- ³³B. J. Skromme, J. Jayapalan, R. P. Vaudo, and V. M. Phanse, *Appl. Phys. Lett.* **74**, 2358 (1999).
- ³⁴K. Pakula, A. Wyszomolek, K. P. Korona, J. M. Baranowski, R. Stepniowski, I. Grzegory, M. Boćkowski, J. Jun, S. Krukowski, M. Wroblewski, and S. Porowski, *Solid State Commun.* **97**, 919 (1996).
- ³⁵O. Lagerstedt and B. Monemar, *J. Appl. Phys.* **45**, 2266 (1974).
- ³⁶S. J. Rhee, S. Kim, E. E. Reuter, S. G. Bishop, and R. J. Molnar, *Appl. Phys. Lett.* **73**, 2636 (1998).
- ³⁷P. W. Yu, C. S. Park, and S. T. Kim, *J. Appl. Phys.* **89**, 1692 (2001).
- ³⁸J. Jayapalan, B. J. Skromme, R. P. Vaudo, and V. M. Phanse, *Appl. Phys. Lett.* **73**, 1188 (1998).
- ³⁹Z. Yang, L. K. Li, and W. I. Wang, *Appl. Phys. Lett.* **67**, 1686 (1995).
- ⁴⁰S. O. Kucheyev, M. Toth, M. R. Phillips, J. S. Williams, C. Jagadish, and G. Li, *J. Appl. Phys.* **91**, 5867 (2002).
- ⁴¹J. Baur, K. Maier, M. Kunzer, U. Kaufmann, J. Schneider, H. Amano, I. Akasaki, T. Detchprohm, and K. Hiramatsu, *Appl. Phys. Lett.* **64**, 857 (1994).
- ⁴²J.-M. Wagner and F. Bechstedt, *Phys. Rev. B* **66**, 115202 (2002).
- ⁴³V. Yu. Davydov, N. S. Averkiev, I. N. Goncharuk, D. K. Nelson, I. P. Nikitina, A. S. Polkovnikov, A. N. Smirnov, M. A. Jacobsen, and O. K. Semchinova, *J. Appl. Phys.* **82**, 5097 (1997).
- ⁴⁴A. Polian, M. Grimsditch, and I. Grzegory, *J. Appl. Phys.* **79**, 3343 (1996).
- ⁴⁵A. R. Goñi, H. Siegle, K. Syassen, C. Thomsen, and J.-M. Wagner, *Phys. Rev. B* **64**, 035205 (2001).